2008 IEEE International Conference on
Robotics and Automation
Pasadena, CA, USA, May 19-23, 2008

Bilateral Energy Transfer in Delayed Teleoperation on the Time Domain

Jordi Artigas, Carsten Preusche and Gerd Hirzinger
Institute of Robotics and Mechatronics
DLR - German Aerospace Center
Germany, Munich
Email: jordi.artigas@dlr.de

Gianni Borghesan and Claudio Melchiorri
Università di Bologna
Bologna, Italy
Email: {gianni.borghesan,claudio.melchiorri}@unibo.it

Abstract— **The time domain passivity framework is attracting interest as a method for granting stability in both telerobotics and haptic contexts; this paper employs this approach in order to introduce a novel concept, the Bilateral Energy Transfer for haptic telepresence. Loosely speaking, the Bilateral Energy Transfer is the straightforward transfer of energy between the two opposite sides of a teleoperation network, the master and slave robots. In an ideal telepresence scenario master and slave robots behave as rigid connected masses [1], and their power exchange is lossless; conversely, realistic scenarios include sources of energy leaks, i.e. elements that modify the power flows in the network. Moreover, if energy leaks have an active nature, they become source of instability for the system. This work isolates two sources of instability normally present in a teleoperation system, i.e. the delayed communication channel and robot velocity estimation based on digital position acquisition. These energy leaks are counterbalanced by two independent controllers, whose design is based on energetic consideration, and whose employment allows to achieve the Bilateral Energy Transfer. The presented arguments are sustained by simulations and experiments.**

I. Introduction

Telepresence is a field that merges telerobotics and haptic concepts, hereby allowing a human operator to control a slave robot located in a remote site by means of a haptic device. The operator becomes therefore an energetically coupled body with the distant environment where a task is to be conducted. While other flows aiming at a realistic and intuitive interaction are normally presented to the user, as visual and aural feedback, the haptic channel is specially challenging due to the inclusion of the human operator in the closed control loop. After stability, the main goal of a telepresence system is transparency, meaning in its ideal form that the user is not able to distinguish remote presence to local presence. Previous works [1], [2] exhaustively explain why the pursuit of stability compromises transparency once the system constraints are established.

One of the most accounted issues in telemanipulation scenarios is the delay in the communication channel, that forces to design conservative control architectures, in order to achieve system stability, thus lowering the system transparency.

Among the most remarkable approaches in dealing with time-delayed telepresence, are those based on the passivity criteria. The appeal of passivity-based approaches is the property that system passivity (and therefore stability) is granted by passivity of its subsystems. Passivity can be proved without need of precise modeling of the analyzed system. Thus it is a useful tool to study a system where some of its elements are difficult to model or unknown, i.e. the human operator, the remote environment, and the communication channel. In particular, the communication channel can be active due to the inclusion of time delay, and the generated energy must be dissipated using some specific technique such as the Scattering transformation [3] and its Wave Variables formulation, [4], which have become classical methods for delayed teleoperation.

These frameworks based on power networks, as Wave Variables or Time Domain Passivity [5], impose the choice of inputs and outputs of the systems as power conjugated variables, i.e. each input is related to an output, their product must be power, and individuates a power port; if the mechanical domain is considered, inputs and outputs must be generalized velocities and torques. Since the robot sensors commonly provide generalized position, the issue of velocity estimation must be tackled before the robot velocity is fed to the discrete controller.

The Time Domain Passivity Control approach, presented in [5], and further applied for delayed scenarios in [6], is here exploited to introduce the concept of *Bilateral Energy Transfer*: To convoy the energy introduced in the master side robot toward the slave robot (and vice versa), as faithfully as possible, with regard to the system passivity. Thus, two main characteristic are sought in the design of the control architecture: To limit unneeded energy dissipation and to convoy, even if with the unavoidable delay due to the transmission delay, the energy. In particular the second design guideline clashes with Wave Variable -based approaches, where power can bounce forth and back in the communication channel, unless some dissipation element is inserted and properly tuned on both sides of the channel [7].

In this paper two sources of energy leaks for the system described in Section II are individuated, the transmission delay and the velocity estimation from sampled position of the robots, both examined in Section III. This two issues are tackled with two different and independent controllers: The **Bilateral Passivity Controller** (BiPC), distributed between Forward and Backward Passivity Controllers (FPC and BPC), which forces the delayed communication channel to passivity, as seen in Section V; and the **Passive Continuous**

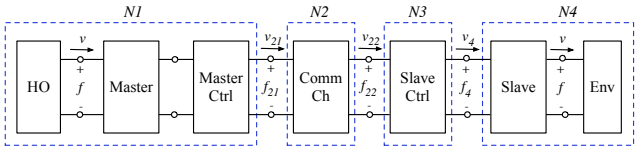

Fig. 1. General network representation of a teleoperation system

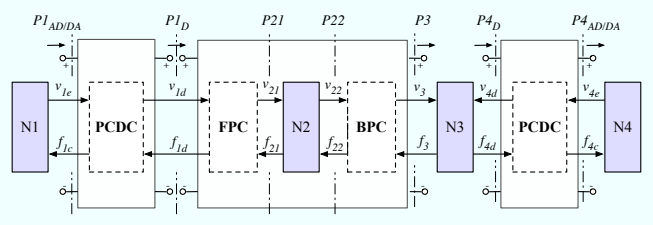

Fig. 2. Network representation of the system including PCDC and FPC / BPC

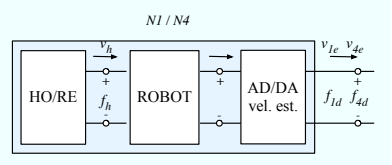

Fig. 3. Close-look of N1/N4

Discrete time Connector (PCDC), which operates on the velocity estimation in order to make the connection between the robots and the digital controller lossless, explained in Section IV. A set of simulations and full setup experiments to analyze the operation and interaction of the passivity controllers are shown in Section VI and in Section VII respectively. Finally, in Section VIII conclusions and future lines are given.

II. System Description

Fig. 1 shows the network representation of a bilateral control system using the mechanical-electrical analogy. This scheme is general and resumes different possible causality choices. Note that both the Human Operator (HO) and the Remote Environment (RE) are considered as part of the system, and are the only admissible sources of energy.

The paper is focused on a particular choice of causality, a velocity - force architecture, shown in Fig. 2. We make use of a dual representation to show mechanical and network equivalences, where the following network arrangements are used throughout the article:

- *N1*: Contains the HO, the master device, and the analog/digital conversion plus the velocity estimation from the robot position (AD/DA - VEL. EST.) (see Fig. 3) . It is usually the source of the system. (1-port).
- *N2*: Is the Communication Channel. (2-port).
- *N3*: Is the Slave Controller. (2-port).
- *N4*: Includes the RE, the slave Robot and its AD/DA - VEL. EST (see Fig. 3). It is usually a passive system. (1-port).
- *PCDC*: The Continuous Discrete time Passive Connector, one at each side (see Sec. IV).
- *FPC and BPC*: Forward and Backward Passivity Controller (see Sec. V).

The Slave Controller (N3) acts as a virtual coupling, tuned in order to grant stability and desired performance in the ideal case, where no delay is present in the control loop and the system is considered in the continuous time domain [6]. (i.e. for a system where the effects of the blocks N2, AD/DA and velocity estimation are null, and the blocks PCDC, FPC / BPC are not present). Note the system does not employ a Master Controller. Instead, the computed force by N3 is applied to both, slave, and master through N2. Fig. 2 also shows the main conjugate signals with their corresponding power port. The following convention with regard to the sign of energy is used; a 1-port element is passive if:

$$E(t) = \int_0^t f(\tau)v(\tau)d\tau + E(0) \geq 0, \qquad (1)$$

where $E(t)$ is the energy of the network, v and f are the port variables denoting velocity entering the block, and force respectively, and $E(0)$ is the energy initially stored in the network at $t = 0$. So in the case the energy source of the system is N1, its energy, $E_{N1}(t)$, traces a negative slope indicating the active behavior.

III. Bilateral energy transfer

As hinted before, the main idea behind this work is the energy transfer from the master side to the slave side of the teleoperation system. The ideal system behaves as two masses, the master and slave robots, connected by the virtual coupling, a spring-damper system; and the energy flows according to this simplified physical model. The introduction of non-idealities brings the system to behave differently, in particular from the point of view of energy flows. In the system presented in Fig. 2, N4 should ideally receive the same amount of energy produced by N1. The energy transfer is however altered by the non-idealities introduced by the communication channel (N2) and the position discretization followed by the velocity estimation AD/DA VEL. EST. By means of the PCDC (Sec. IV) and the BiPC (Sec. V), the Bilateral Energy Transfer presented in this article tries to diminish these energy leaks so that the system behaves as close as possible to the ideal case.

A. Effects of Discretization

Time discretization is a well known cause of energy generation extensively investigated in the field of haptic interface control, as in [8], [9]. Moreover, the control schemes based on the passivity approach, and in general on power ports representation, need a velocity input, while most of the robots are equipped with position sensors, thus velocity must be estimated. When the position signal is discretized, the only information that can be retrieved on velocity is the *average* velocity of the *previous* sample time. If the velocity is approximated by means of this method, there is a difference

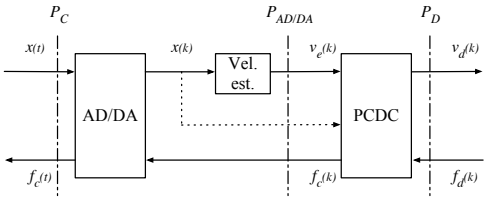

Fig. 4. Velocity estimation from sampled position and PCDC element

of incoming and outcoming energy $\Delta E_{err}(k)$ in each sample time $t \in [kT_s, (k+1)T_s)$ of length T_s.

$$\Delta E_{err}(k) = T_s\, f_d(k)\big(v_e(k) - v_e(k-1)\big) \tag{2}$$

where $v_e(k) = (x(k+1) - x(k))/T_s$, is the average velocity of the robot, $x(k)$ the robot position sampled at $t = kT_s$, and $f_d(k)$ the force feed by the discrete controller to the robot. Note that $\Delta E_{err}(k)$ can be computed only at $t = (k+1)T_s$.

B. Effects of Time Delay

It is widely known that the presence of transmission delays strongly compromises the stability of a system. From an energetic point of view, the two ports element (N2) created by the delayed channel generates or dissipates power since

$$v_{21}(t)f_{21}(t) - v_{22}(t)f_{22}(t) \neq 0, \tag{3}$$

where $v_{21}(t)$, $f_{21}(t)$, $v_{22}(t)$ and $f_{22}(t)$ denote velocity and force signals from N2 observed at port $P21$ and $P22$ respectively, i.e. the power conjugate variables of N2 (see Fig. 2). Furthermore, the signals are related as:

$$v_{22}(t) = v_{21}(t-T), \qquad f_{21}(t) = f_{22}(t-T). \tag{4}$$

N2 acts as a source of energy and can insert energy to one side or to the other depending on the behavior of N1 and N4. The expression of energy of N2 considering the flow from left to right is:

$$\begin{aligned} E_{N_2}(t) = \int_0^t & f_{22}(\tau)(-v_{22}(\tau)) \\ & - [f_{21}(\tau)(-v_{21}(\tau))]d\tau + E_{N2}(0), \end{aligned} \tag{5}$$

which becomes negative if N1 is active and N4 passive. Note that both velocities are negated conforming with the convention in (1). In Fig. 7(e) the effect upon energy of a (controlled) communication delay of $400ms$ on N2 can be seen. Furthermore, relating equations (4) and (5), the natural active behavior of the delayed network can be proved. This active nature can also be proved by describing the network element with the scattering parameters as in [3].

IV. Passive Continuous Discrete time Connector

The same rationale behind the solution proposed in [10] for passively interconnecting multi-rate systems is adopted for dealing with the problem of energy generation due to the discretization of position information. The result is an element, called PCDC (Passive Continuous Discrete time Connector), which connects the sampled data coming from the haptic interface to a discrete time systems. As the Passivity Observer / Passivity Controller, this element observes the power flows and modifies one of its output in order to minimize the power generation (or dissipation) due to time discretization and velocity estimation. The PCDC (Fig. 4) has three inputs, the force coming from the discrete time controller $f_d(k)$, the sampled positions $x(k)$ of the haptic interface, and the estimated velocity $v_e(k)$. It also has two outputs, the velocity going to the controller $v_d(k)$ and the force to the haptic interface $f_c(k)$. This system also keeps track of the energy error $E(k)$. Over a sample period of length T_s, the energy balance of the system given by the port interconnection of the AD/DA and the PCDC, (whose ports are referred as continuous (P_C) and discrete (P_D) in (Fig. 4)) is:

$$\begin{aligned} \Delta E(k) &= \int_{kT_s}^{(k+1)T_s} \dot{q}(t)f_c(t)dt - T_s f_d(k)v_d(k) \\ &= (x(k+1) - x(k))f_c(k) - T_s f_d(k)v_d(k), \end{aligned} \tag{6}$$

where $f_c(t)$, obtained holding $f_c(k)$, is the continuous time force signal fed to the robot. As already pointed out in [9], it is the possible to compute the net energy flow $\Delta E(k)$ only at $t = (k+1)T_s$; the energy error accumulated inside the PCDC system is given by:

$$E(k+1) = E(k) + \Delta E(k), \quad E(0) = 0 \tag{7}$$

The output $f_c(k)$ and $v_d(k)$ are chosen as

$$f_c(k) = f_d(k) \tag{8}$$

$$v_d(k) = v_e(k) + \Delta P(k)/f_d(k) \tag{9}$$

where $v_e(k) = (x(k) - x(k-1))/T_s$ the estimated velocity, and $T_s\Delta P(k)$ is the energy that flows from the stored energy $E(k)$ to the discrete port in a sample time; In order to avoid an excessive distortion of the velocity signal in critical situation (i.e. when $f_d(k) \simeq 0$), some limit conditions must be imposed to the maximum value of $|\Delta P(k)|$; this bound is expressed by:

$$|v_d(k) - v_d(k-1)| \leq |v_e(k) - v_e(k-1)|, \tag{10}$$

which leads to

$$\left| v_e(k) + \frac{\Delta P(k)}{f_d(k)} - v_d(k-1) \right| \leq |v_e(k) - v_e(k-1)| \tag{11}$$

thanks to (9). After applying the *inverse triangular equation* to (11) and simple calculations, the following upper bound to $\Delta P(k)$ is found:

$$\left| \frac{\Delta P(k)}{f_d(k)} \right| \leq |v_e(k) - v_e(k-1)| + |v_e(k) - v_d(k-1)|. \tag{12}$$

Since the energy supplied to the discrete port must not exceed the stored one the following condition also applies:

$$T_s\Delta P(k) \leq |E(k+1)| \tag{13}$$

$$\text{sign}(\Delta P(k)) = \text{sign}(E(k+1)) \tag{14}$$

The value assigned to $\Delta P(k)$ is, in absolute value, the maximum allowed by (12) and (13), and the sign is computed by (14).

V. Backward and Forward Passivity Controllers

Equation (5) shows the energy balance of N2. As discussed in [6], the discrete energy of a communication channel element,

$$E_{N_2}(n) = \Delta T_s \left[\sum_{k=0}^{n} f_{22}(k)(-v_{22}(k)) - f_{21}(k)(-v_{21}(k)) \right], \tag{15}$$

is not observable in real time, since the conjugate pairs (v_{21}, f_{21} and v_{22}, f_{22}) in (15) should be simultaneously available at one of the two sides; instead, the following approximation for the energy flow from left to right in the discrete time can be registered at the right port of N2:

$$E^*_{N_{2R}}(n) = E_{bwd}(n) - E^*_{P21}(n), \tag{16}$$

$$E_{bwd}(n) = \Delta T_s \sum_{k=0}^{n} f_{22}(k)(-v_{22}(k)), \tag{17}$$

$$E^*_{P21}(n) = \Delta T_s \sum_{k=0}^{n-T} f_{21}(k)(-v_{21}(k)), \tag{18}$$

where $E_{bwd}(n)$ represents the energy coming out of the channel from port $P22$ (this is equivalent to observe the 1-port network created by N1, N2, the left PCDC and FPC), and $E^*_{P21}(n)$ represents the energy entering in the channel through port $P21$ but delayed T seconds. Using the same principle as in [6], the Backward Passivity Controller (BPC) configured with admittance causality is inserted between N2 and N3. The BPC monitors the energy $E^*_{N_{2R}}$ and introduces a dissipative element with dissipation E_{bpc} which assures that the energy flow from $P21$ to $P3$, $E_{N_{2R}}$, will not drop below zero. This is:

$$E_{N_{2R}}(n) = E_{bwd}(n) - E_{ref}(n) + E_{bpc}(n) \geq 0, \tag{19}$$

where

$$E_{ref}(n) = \begin{cases} E^*_{P21}(n) & \text{if } E^*_{P21}(n) < 0 \text{ (active)} \\ 0 & \text{if } E^*_{P21}(n) \geq 0. \end{cases} \tag{20}$$

If N2 becomes active the difference $E_{bwd}(n) - E_{ref}(n)$ turns negative. This triggers the BPC which in turn slows down the system, i.e. dissipates the energy introduced by the channel, by means of the coefficient α_{bpc}, so that:

$$v_3(n) = v_2(n) - \frac{f_2(n)}{\alpha_{bpc}(n)}, \qquad f_{22}(n) = f_3(n), \tag{21}$$

$$\frac{1}{\alpha_{bpc}(n)} = \frac{-[E_{bwd}(n) - E_{ref}(n) + E_{bpc}(n-1)]}{f_3(n)^2}, \tag{22}$$

and as a result, the dissipated energy:

$$E_{bpc}(n) = \Delta T_s \sum_{k=0}^{n} \frac{1}{\alpha_{bpc}(k)} f_3(k)^2 \geq -E_{bwd}(n) + E_{ref}(n). \tag{23}$$

The computation of α_{bpc} and, in general, the action of the BPC, follows a similar strategy as the one used in [11], and can be understood as a 1-port Passivity Controller with an energetic reference, where the controlled port is $P3$ with E_{bwd}, and the reference, E_{ref}, is the active energy displayed at $P21$. Depending on the active/passive character of E_{ref} and E_{bwd} the BPC will dissipate channel energy or not. For instance, if N1 is the source and the delay $T = 0$, both, E_{bwd} and E_{ref}, will be negative (active) but equal. The BPC will therefore not be activated. If N1 is source and the delay $T > 0$, both, E_{ref} and E_{bwd} may become active (negative), and $|E_{bwd}| > |E_{ref}|$. This is the typical situation where channel energy flows from left to right, and therefore the BPC will be activated and dissipate the activity of $E_{N_{2R}}(n)$. Table I synthesizes the operation of the BPC[1] [2].

TABLE I
Operation of the BPC

Src.	Delay (T)	Energy Condition	$\frac{1}{\alpha_{bpc}(n)}$	Descr.
N1	0	$E_{bwd} < 0$, $E^*_{P21} < 0$ ($E_{bwd} = E^*_{P21}$)	Off	N2 is lossless
N1	> 0	$E_{bwd} < 0$, $E^*_{P21} < 0$ ($\|E_{bwd}\| > \|E^*_{P21}\|$)	On	N2 is active from L2R
N1	> 0	$E_{bwd} < 0$, $E^*_{P21} > 0$	On	N2 is active from L2R
N4	0	$E_{bwd} > 0$, $E^*_{P21} > 0$ ($E_{bwd} = E^*_{P21}$)	Off	N2 is transparent
N4	> 0	$E_{bwd} > 0$, $E^*_{P21} > 0$ ($\|E^*_{P21}\| > \|E_{bwd}\|$)	Off	N2 is active from R2L
N4	> 0	$E_{bwd} < 0$, $E^*_{P21} > 0$	Off	N2 is active

If N4 has an active behavior, N2 may exhibit an active behavior at port $P21$ as well. Therefore the Forward Passivity Controller (FPC) is inserted at the left of N2 configured with impedance causality, and, in analogy with the BPC, it observes the energy flow from right to left and avoids activity in this direction.

One issue when using BPC and FPC is the error present between real and observed channel energy. For BPC case this can be seen comparing (15) and (16). The error is given by:

$$\begin{aligned} E_{N2Rerr} &= E_{N_2}(n) - E^*_{N_{2R}}(n) \\ &= -\Delta T_s \sum_{k=n-T}^{n} f_{21}(k) v_{21}(k) \end{aligned} \tag{24}$$

There are different alternatives to deal with that error; in [6] the error is allowed and the damping parameter of the virtual coupling is tuned experimentally in order to dissipate the energy of the error; however, since the error only depends on v_{21} and f_{21}, E_{N2Rerr} can be predicted on the left side of the N2, but its computation requires a priori knowledge of time delay T.

VI. Simulation

The master and slave robots are simulated (Matlab Simulink) as mass-damper systems with mass $M_r = 1\,Kg$

[1] *The Source* in Table I (N1 / N4) gives an approximate idea of the general behavior of the system and does not determine the operation of the BPC / FPC. For instance, it is possible that N4 acts as a source and N2 shows an energy flow from left to right.

[2] L2R and R2L stand for *left to right* and *right to left*

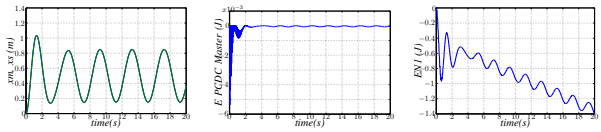

(a) M-S Positions (b) PCDC M. Energy (c) Master Energy

Fig. 5. Experiment with $T_{rt} = 0.004$, $K_c = 15500$, $B_c = 10.4$ a) Master/slave positions. b) Master PCDC energy, $E_{P1_D} - E_{P1_{AD/DA}}$. c) Master energy, E_{P1_D}.

and viscous friction of $B_r = 0.3\,Ns/m$. The HO is simulated in a closed-loop system that generates the force to the master robot in order to follow a sinusoidal reference position with frequency of $0.25\,Hz$ and amplitude of $0.25\,m$. The control part of the system (PCDCs, FPC, BPC and N3) runs at a sampling time of $T_s = 1\,ms$. The virtual coupling (N3) is obtained by discretization of a continuous time PI controller with gains K_c and B_c; the plot in Figs. 5, 6 and 7 refer to the energy E_{Px} flowing from left to right through the ports Px as defined in Fig. 2.

A. Small delay - Influence of the PCDC

Using a fixed small delay ($T = 4\,ms$) the gain K_c of N3 has been increased until the system, with both PCDCs deactivated, goes to instability, resulting in a stiffness of roughly $5000\,N/m$, while B_c has been fixed to $10.4\,Ns/m$. the same test has been done switching on the PCDCs, obtaining stability with a stiffness up to three times greater. Fig. 5 shows the master and slave positions, and energies in various parts of the network; in particular, Fig. 5(b) refers to the master and slave positions (x_m, x_s), that are overlapped. Fig 5(b) shows that the energy error in the master PCDC, that is several order of magnitude smaller than the energy provided from the master robot at Port $P1_D$, Fig. 5(c).

B. Delayed teleoperation - Combined PCDC and BiPC

Figures 6 and 7 show the results obtained by two simulations of a delayed teleoperation. The simulations are run with a round trip delay of $T_{rt} = 0.4\,s$ (where $T_{rt} = 2T$), a virtual coupling stiffness of $K_c = 3500\,N/m$ and damping of $B_c = 10.4\,N/m$. The system becomes thus highly unstable if not controlled with the BPC and FPC. The PCDCs are deactivated in the first simulation (Fig. 6) and activated in the latter (Fig. 7). The effects of the PDCDs can be evaluated by difference of energy that is injected into the system (Figs. 6(c), 7(c)). Previous work presented in [6] could achieve stability as well. However the constants of the virtual coupling had to be tuned in order to cope with the error introduced by (19) and the energy leak injected by the AD/DA - VEL. EST. In Figs. 6(e), 6(f) and Figs. 7(e), 7(f) it is possible to compare the energy of the channel N2 before any correction (Ports P21, P22) and after the correction operated by the BPC (Ports P21, P3). It is possible to see how the BPC is able to correct the active behavior of the channel (being E_{N2} in Figs. 6(e), 7(e) negative) to a passive behavior (Figs., 6(f), 7(f)).

These simulations show how efficient is the combined use of the BiPC and PCDCs, in order to capture a faithful

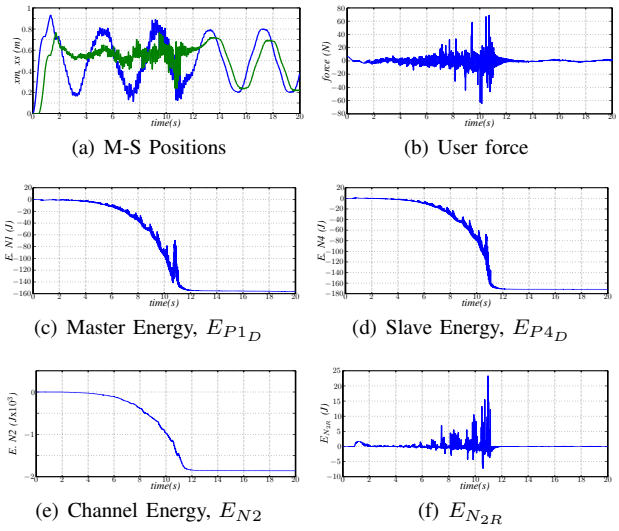

(a) M-S Positions (b) User force

(c) Master Energy, E_{P1_D} (d) Slave Energy, E_{P4_D}

(e) Channel Energy, E_{N2} (f) $E_{N_{2R}}$

Fig. 6. Simulation with $T_{rt} = 0.400$, $K_c = 3500$, $B_c = 10.4$

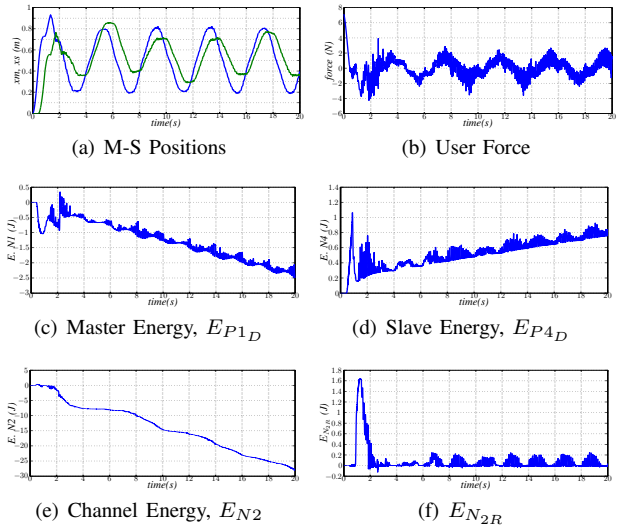

(a) M-S Positions (b) User Force

(c) Master Energy, E_{P1_D} (d) Slave Energy, E_{P4_D}

(e) Channel Energy, E_{N2} (f) $E_{N_{2R}}$

Fig. 7. Simulation with $T_{rt} = 0.400$, $K_c = 3500$, $B_c = 10.4$, PCDC.

measurement of the energy injected by the user and to be conveyed to the other side of communication channel, thus resulting in an effective Bilateral Energy Transfer.

VII. Experiments

The setup uses the same control scheme employed in the simulations of Sec. VI. The master and slave systems consist of a LWR III and LWR II respectively (Fig. 10). These are 6 DoF Light Weight Robots with masses of around 20 Kg. developed in the DLR (German Aerospace Center). The LWR III includes a joystick handler as end effector and both robots are real time driven by QNX at a sampling rate of 1 kHz. The communication channel is a UDP connection where a circular buffer was implemented in order to simulate a wide variety of time delays. As previously the BPC operates on the velocity fed to N3 and FPC on the force fed to N1. Two experiments, with different delays are here presented; the data shown in Fig. 8 has been collected using a round trip delay of $T_{rt} = 200\,ms$, and Fig. 9 refers to

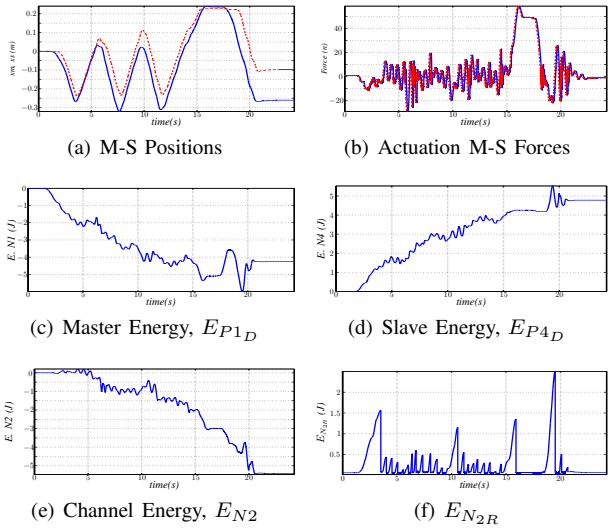

(a) M-S Positions (b) Actuation M-S Forces

(c) Master Energy, E_{P1_D} (d) Slave Energy, E_{P4_D}

(e) Channel Energy, E_{N2} (f) $E_{N_{2R}}$

Fig. 8. Experimental data with $T_{rt} = 200\,ms$

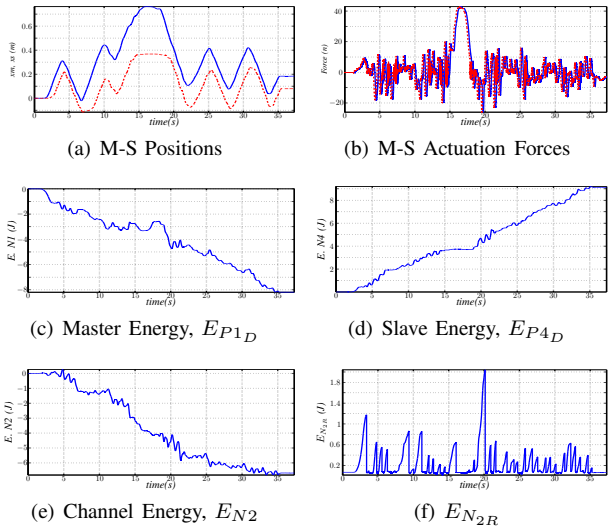

(a) M-S Positions (b) M-S Actuation Forces

(c) Master Energy, E_{P1_D} (d) Slave Energy, E_{P4_D}

(e) Channel Energy, E_{N2} (f) $E_{N_{2R}}$

Fig. 9. Experimental data with $T_{rt} = 400\,ms$

$T_{rt} = 400\,ms$. The system has been experimentally proved to be highly unstable (with delays starting from $T_{rt} = 30\,ms$) if BiPC - PCDC are not used. It can be seen that the experiments follow similar patterns as in the simulation, with the only notable exception that the forces represented in Figures 8(b) and 9(b) are the forces imposed to the low level controllers which in turn compute the robot actuator torques; Since the user actively moves the LWR III, N1 becomes the main energy source while N4 behaves passive. The channel, N2, mostly generates energy toward the slave side. Therefore the BPC is triggered frequently, modifying the velocity (and causing part of the position drift) while the FPC is activated less often. If the slave robot is used as an interface, so that the energy is injected from N4 and transmitted to N1, the symmetric behavior of BiPC occurs, i.e. N2 generates energy toward N1, FPC dissipates this energy, while the BPC is less active. Both experiments show that the system retains stability in both, free space and contacting with a stiff wall.

Fig. 10. Experimental setup

VIII. Conclusion

The work here presented tackles the problem of delayed haptic telepresence using novel control strategies based on real time energetic consideration. The benefits of employing real time energetic control, i.e. Time Domain Passivity, are here corroborated allowing us to neutralize damaging effects introduced by the unavoidable non-idealities of the system. The twofold controller strategy limits energy generated by position sampling and derivation processes, and makes the delayed communication channel passive. A traditional force-velocity teleoperation scheme, whose original stability regions swept upon communication delay were found to be extremely narrow, has now been equipped with two PCDCs and the BiPC. The new system augments its stability regions and is able to bear significant time delays. Both simulation and experiments show how the conjunction of BiPC and the PCDCs make possible a more accurate Bilateral Energy Transfer, which in turn outcomes in higher transparency. In particular, the control action of PCDCs allows a more relaxed operative conditions for the BiPC, that are triggered less frequently and dissipate less energy. As a last remark, it is worth to point out that the BiPC can be adapted with small efforts to an asymmetrical varying communication channel delay, as will be shown in future works.

References

[1] Y. Yokokohji and T. Yoshikawa, "Bilateral Control of Master-Slave Manipulators for Ideal kinesthetic Coupling – Formulation and Experiment," *IEEE Transactions on Robotics and Automation*, vol. 10, no. 5, pp. 605–620, October 1994.

[2] D. A. Lawrence, "Stability and transparency in bilateral teleoperation," *IEEE Transactions on Robotics and Automation*, vol. 9, no. 5, 1993.

[3] R. J. Anderson and M. W. Spong, "Bilateral control of teleoperators with time delay," *IEEE Transactions on Automatic Control*, vol. 34, no. 5, pp. 494–501, May 1989.

[4] G. Niemeyer, "Using wave variables in time delayed force reflecting teleoperation," Ph.D. dissertation, Massachussetts Institute of Technology, Sept. 1996.

[5] B. Hannaford and J.-H. Ryu, "Time domain passivity control of haptic interfaces," in *Proc. IEEE ICRA '01*, 2001, pp. 1863–1869.

[6] J. Artigas, C. Preusche, and G. Hirzinger, "Time domain passivity for delayed haptic telepresence with energy reference," in *Proc. IEEE/RSJ IROS'07.*, San Diego, CA, USA, 2007.

[7] C. Secchi, S. Stramigioli, and C. Fantuzzi, *Control of interactive robotic interfaces A port-Hamiltonian approach*, ser. Springer Tracks in advanced robotics, B. Siciliano, O. Khatib, and F. Groen, Eds. New York: Springer Verlag, 2007, vol. 29.

[8] J. J. Abbot and A. M. Okamura, "Effects of position quantization and sampling rate on virtual-wall passivity," *IEEE Trans. on Robotics*, vol. 21,5, pp. 952 – 964, 2005.

[9] B. Hannaford, J.-H. Ryu, and Y. S. Kim, "Sampled- and continuous-time passivity and stability of virtual environments," *IEEE Trans. on Robotics*, vol. 20,4, pp. 772– 776, 2004.

[10] G. Borghesan, A. Macchelli, and C. Melchiorri, "Simulation issues in haptics," in *Proc. IEEE ICRA '07*, 2007.

[11] J.-H. Ryu, B. Hannaford, C. Preusche, and G. Hirzinger, "Time Domain Passivity Control with Reference Energy Behavior," in *Proc. IEEE/RSJ IROS'03*, Las Vegas, Nevada, USA, October 2003.